Syntheses, Crystal Structures and Reactivity of Organometallic Tantalum(IV) Phosphinidene Complexes: *trans*-[{Cp*TaCl(μ-PR)}$_2$] (Cp* = C_5Me_5, R = Cy, *t*Bu, Ph), *cis*- and *trans*-[{Cp*TaCl(μ-PMes)}$_2$] (Mes = 2,4,6-$Me_3C_6H_2$) and *cis*-[{Cp′TaCl(μ-PMes)}$_2$] (Cp′ = C_5H_4Me)

Steffen Blaurock[a] and Evamarie Hey-Hawkins*[a]

Keywords: Tantalum / P ligands / Oxo ligands / Isocyanide ligands

The reaction of [Cp*TaCl$_4$] (Cp* = C_5Me_5) with LiPHR (1:1 or 1:2) gives the phosphinidene-bridged tantalum(IV) complexes *trans*-[{Cp*TaCl(μ-PR)}$_2$] [R = Cy (**1**), *t*Bu (**2**), Ph (**3**), 2,4,6-$Me_3C_6H_2$ (Mes) (**4b**)]. When the reaction with LiPHMes is carried out in a 1:1 ratio, *cis*-[{Cp*TaCl(μ-PMes)}$_2$] (**4a**) is also formed besides **4b**. For comparison, *cis*-[{Cp′TaCl(μ-PMes)}$_2$] (**5**) was prepared from [Cp′TaCl$_4$] (Cp′ = C_5MeH_4) and LiPHMes (1:1). **1**–**5** are diamagnetic and were characterised spectroscopically (IR, MS; ^{1}H, ^{31}P, ^{13}C NMR). Crystal structure determinations on **1**–**5** showed the presence of dimeric phosphinidene-bridged Ta^{IV} complexes. The phosphinidene-bridged complexes **1**, **3** and **4b** do not react with acetone, benzophenone, acetonitrile, CS_2 (**1**, **3**), acetaldehyde (**4b**), or ethylaluminum dichloride (**3**). **3** reacts with moist acetone in the presence of traces of air to give the trinuclear cluster [{Cp*TaCl(μ$_2$–O)}$_3$(μ$_3$-O)(μ$_2$-O_2PHPh)] (**6**) in very low yield. With an excess of CyNC, **3** gives [Cp*TaCl(CNCy)$_4$]Cl (**7**), which was characterised by ^{1}H and ^{13}C NMR spectroscopy and by crystal structure determination. As a minor product, [(Cp*TaCl$_2$)$_2$(μ$_2$-O)(η^2,μ$_2$-P_2Cy_2)] (**8**) was also obtained in the reaction of [Cp*TaCl$_4$] with LiPHCy. **6** and **8** were only characterised by crystal structure determination.

Introduction

Organometallic dialkyl- and diarylphosphanido complexes of early transition metals have been studied intensively, while complexes derived from functionalised phosphanes which exhibit a reactive phosphorus-ligand bond have largely been neglected.[1] To date, only a few phosphanido derivatives of organometallic[2,3] and inorganic[4,5] tantalum compounds, one phosphinidene-bridged dimeric Ta^{IV} complex[3] and two stable terminal phosphinidene complexes[5,6] have been described in the literature.

Recently, we reported the syntheses and structures of the primary phosphane complexes [Cp′TaCl$_4$(PH$_2$Tipp)] (Cp′ = C_5H_4Me, Tipp = 2,4,6-*i*Pr$_3$C$_6$H$_2$)[3] and [Cp*MCl$_4$(PH$_2$R)] [Cp* = C_5Me_5; M = Nb, Ta; R = *t*Bu, Ad, Cy, Ph, 2,4,6-$Me_3C_6H_2$ (Mes)],[7] which we expected to be suitable precursors for the preparation of phosphanido and phosphinidene complexes. However, when [Cp*TaCl$_4$(PH$_2$R)] (R = *t*Bu, Cy, Ad, Ph, Mes) were treated with DBU an internal redox reaction occurred with formation of [(DBU)H][Cp*TaCl$_4$] (DBU = 1,8-diazabicyclo[5.4.0]undec-7-ene) and the corresponding diphosphane ($P_2H_2R_2$) or decomposition products thereof.[8] For the aryl-substituted phosphane complexes, there was also an indication from the ^{31}P NMR spectra of the formation of tantalum phosphinidene complexes, which could, however, not be isolated.

We now report the targeted synthesis of these and other dimeric Ta^{IV} phosphinidene complexes, which are accessible from [Cp^{R}TaCl$_4$] (Cp^R = Cp*, Cp′) and LiPHR′, and some reaction products thereof. The related tantalum(IV) phenylimido complex *trans*-[{Cp*TaCl(μ-NPh)}$_2$] is also known.[9]

Results and Discussion

Synthesis and Properties of *trans*-[{Cp*TaCl(μ-PR)}$_2$] [R = Cy (1), *t*Bu (2), Ph (3)], *cis*- and *trans*-[{Cp*TaCl(μ-PMes)}$_2$] (4a,b) and *cis*-[{Cp′TaCl(μ-PMes)}$_2$] (5)

When [Cp*TaCl$_4$][7,10] was treated with two equivalents of LiPHR[11–14] in toluene (to keep the concentration of LiPHR low in solution) at low temperature (to reduce side reactions), the deep red phosphinidene-bridged tantalum(IV) complexes *trans*-[{Cp*TaCl(μ-PR)}$_2$] [R = Cy (**1**), *t*Bu (**2**), Ph (**3**), Mes (**4b**)] were obtained after workup in 73 to 86% yield (based on [Cp*TaCl$_4$]; Scheme 1).

In the ^{31}P NMR spectra of the reaction mixtures, one singlet is observed for the *t*Bu, Ph and Mes derivatives, while for the Cy derivative, two singlets are observed in the low-field region, one of which has only a low intensity [δ = 437.6 (major) and 433.7 (minor) ppm]. The major signal

[a] Institut für Anorganische Chemie der Universität Leipzig
Johannisallee 29, 04103 Leipzig (Germany)
Fax: (internat.) + 49–(0)341/9739319
E-mail: hey@rz.uni-leipzig.de

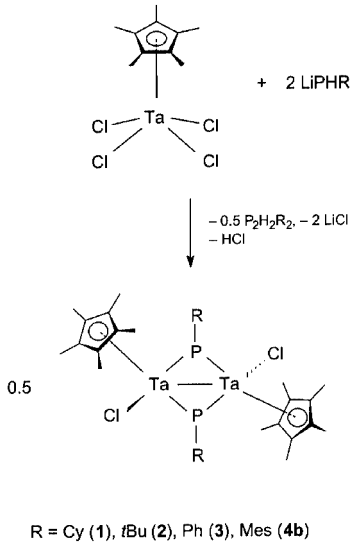

Scheme 1

was shown to belong to the *trans* isomer, while the minor signal presumably belongs to the *cis* isomer.

When the reaction of [Cp*$TaCl_4$] with LiPHMes was carried out in a 1:1 ratio, *cis*-[{Cp*TaCl(μ-PMes)}$_2$] (**4a**) was also formed along with **4b**. An additional signal was observed in the ^{31}P NMR spectrum at δ = 485.8 ppm [ratio ca. 1 (**4a**): 6 (**4b**): 3], which indicates the formation of a terminal phosphinidene complex, [Cp*$TaCl_2$(PMes)] (cf. the stable terminal phosphinidene complex [Cp*$TaCl_2${P(Tipp)}], which shows a singlet at δ = 488.0 ppm).[15] The mesitylphosphinidene complex could, however, not be obtained in its pure form. Complexes **4a** and **4b** could be separated by fractional crystallisation from *n*-hexane.

For comparison, *cis*-[{Cp′TaCl(μ-PMes)}$_2$] (**5**) was prepared from [Cp′$TaCl_4$][16] and LiPHMes (1:1). In the ^{31}P NMR spectrum of the reaction mixture, only one signal was observed, which indicates the exclusive formation of the *cis* isomer.

In these reactions, the lithium reagent acts as a reducing agent, base and substitution reagent. The products of these reactions, that is, the oxidation product $P_2H_2R_2$, the free phosphane RPH_2, and the corresponding Ta^{IV} phosphinidene complex were detected by ^{31}P NMR spectroscopy.

The formation of **1**–**4b** was also observed when only one equivalent of LiPHR was used, but the yield was lower.

Related tantalum phosphinidene complexes include *trans*-[(Cp′TaCl{μ-P(Tipp)})$_2$] (**I**),[3] which was obtained by treating [Cp′$TaCl_4${PH_2(Tipp)}] with DBU (1:2 or 1:3), and the stable terminal phosphinidene complexes [N{$CH_2CH_2N(SiMe_3)$}$_3$Ta=PR] [δ(^{31}P) = 175.1 (R = Cy) and 227.3 (R = *t*Bu) ppm][6] and [(tBu$_3$SiO)$_3$Ta=PPh][5] [δ(^{31}P) = 334.6 ppm]. These ^{31}P chemical shifts indicate the presence of a linear MPR unit (bent MPR unit: δ = 660 to 800 ppm).[17] For **1**–**5** and **I**, ^{31}P chemical shifts of δ = 390.3 ppm (for **4b**) to 482.0 ppm (for **2**) are observed [for **I**, δ(^{31}P) = 391.5 ppm], and Δδ (phosphane vs. phosphinidene complex) ranges from δ = 526 to 562 ppm (Table 1).

Apparently, the influence of the substituted cyclopentadienyl ligand on the ^{31}P NMR chemical shift is negligible, as shown by the similar values for **4b** (Cp* complex) and **I** (Cp′ complex), while alkyl-substituted phosphinidene complexes **1** and **2** exhibit low-field shifts compared to aryl-substituted phosphinidene complexes **3**–**5**. The same trend is observed for the corresponding primary phosphanes (Table 1).

In the ^{13}C NMR spectra of **1**–**4**, the signals of the carbon atoms of the Cp* ring are shifted to high field by Δδ = 16.5–18 relative to the starting material [Cp*$TaCl_4$] (δ = 132.9 ppm).

Molecular ion peaks were observed in the mass spectra of **1**–**4**.[18] For **1**, **3**, and **4a**, signals for monomeric [Cp*TaCl(PR)]$^+$ and fragmentation products thereof were also observed.

In the UV/Vis spectra in pentane, **1**–**4** exhibit four absorptions in the ranges 682 – 753 (ν_1), 473 – 528 (ν_2), 337 – 396 (ν_3), and 313 – 319 nm (ν_4), with molar absorption coefficients of 10^2 – 10^3 (for ν_1, d-d transition), $2{\cdot}10^3$ – 10^4 (for ν_2 and ν_3; CT transitions), and 10^4 – $3{\cdot}10^4$ cm^2/mol (for ν_4, π -π * transition of Cp*).

Molecular Structures of *trans*-[{Cp*TaCl(μ-PR)}$_2$] [R = Cy (1), *t*Bu (2), Ph (3), Mes (4b)], *cis*-[{Cp*TaCl(μ-PMes)}$_2$] (4a) and *cis*-[{Cp′TaCl(μ-PMes)}$_2$] (5)

Single crystals of **1**–**5** were obtained from concentrated solutions in diethyl ether (**1**, **3**), pentane (**2**) or hexane (**4a**,**b**, **5**) at 5 °C. The *trans* complexes **1**–**3** crystallise in the monoclinic space group $P2_1/n$, **4b** in the monoclinic space group $P2_1/c$ and have two formula units per unit cell; the *cis* complexes **4a** and **5** crystallise in the triclinic space group $P\bar{1}$ with two formula units in the unit cell (Table 2). The unit

Table 1. Comparison of the ^{31}P NMR spectroscopic data of compounds **1**–**5** and [(Cp′TaCl{μ-P(Tipp)})$_2$] (**I**)[3] (NMR in C_6D_6) with the ^{31}P{^{1}H} NMR spectroscopic data of the corresponding primary phosphanes

	1 (*trans*) R = Cy	**2** (*trans*) R = tBu	**3** (*trans*) R = Ph	**4a** (*cis*) R = Mes	**4b** (*trans*) R = Mes	**5** (*cis*) R = Mes	**I** (*trans*)
δ(^{31}P, ppm)	437.6	482.0	403.9	399.0	390.3	396.0	391.5
	PH_2Cy[39]	PH_2Bu[36b]	PH_2Ph[36b]	PH_2Mes[36b,40,41]	PH_2Mes[36b,40,41]	PH_2Mes[36b,40,41]	PH_2(Tipp)[36b]
δ(^{31}P, ppm)	–111.3	–80.5	–122.1	–153.8	–153.8	–153.8	–158.2
Δ δ	549.0	562.4	526.0	552.8	544.1	549.8	549.7

Table 2. Crystal data and structure refinement for **1**–**8**

Compound	**1**·2Et$_2$O	**2**	**3**	**4a** (*cis*)	**4b**
Empirical formula	$C_{36}H_{62}OCl_2P_2Ta_2$	$C_{28}H_{48}Cl_2P_2Ta_2$	$C_{32}H_{40}Cl_2P_2Ta_2$	$C_{38}H_{52}P_2Cl_2Ta_2$· hexane	$C_{38}H_{52}P_2Cl_2Ta_2$
Molecular mass	1005.76	879.40	919.38	1003.54	1003.54
Temperature [K]	220(2)	220(2)	220(2)	220(2)	220(2)
Crystal system	monoclinic	monoclinic	monoclinic	triclinic	monoclinic
Space group	$P2_1/n$ (no. 14)	$P2_1/n$ (no. 14)	$P2_1/n$ (no. 14)	$P\bar{1}$ (no. 2)	$P2_1/c$ (no. 14)
Unit cell dimensions					
a [Å]	12.168(2)	12.386(3)	8.813(2)	8.7270(3)	11.1373(5)
b [Å]	9.219(2)	9.288(2)	13.214(3)	12.6329(4)	9.7817(4)
c [Å]	18.841(4)	14.166(3)	14.724(3)	21.2748(8)	17.5396(8)
α [°]	90	90	90	104.018(1)	90
β [°]	106.95(3)	96.25(3)	105.53(3)	91.234(1)	90.052(1)
γ [°]	90	90	90	99.577(1)	90
V [Å^3]	2021.7(7)	1619.9(6)	1652.1(6)	2239.2(2)	1910.8(2)
Z	2	2	2	2	2
$\rho_{calcd.}$ [g cm^{-3}]	1.556	1.803	1.848	1.552	1.744
μ(Mo-K_α) [mm^{-1}]	5.644	7.029	6.897	5.099	5.971
F(000)	972	852	884	1030	980
$\Theta_{min.}$, Θ_{max} [°]	1.78–24.74	2.08–27.93	2.11–27.86	1.73–28.54	1.83–27.85
Index ranges					
	−13 h 13	−15 h 14	−11 h 11	−11 h 11	−14 h 10
	−10 k 10	−12 k 11	−17 k 9	−8 k 16	−12 k 12
	−21 l 18	−18 l 17	−19 l 19	−27 l 28	−20 l 21
Reflections collected	8166	14304	9194	13684	
Independent reflections	3295	3601	3568	9902	4145
R(int)	0.0182	0.0405	0.0336	0.0186	0.0430
Parameters	240	178	237	432	281
Goodness-of-fit on F^2	0.974	1.060	1.029	0.946	1.029
Final R indices [$I > 2\sigma(I)$]					
R_1	0.0275	0.0228	0.0269	0.0290	0.0364
wR_2	0.0747	0.0554	0.0631	0.0911	0.0860
R indices (all data)					
R_1	0.0301	0.0267	0.0360	0.0406	0.0572
wR_2	0.0798	0.0575	0.0679	0.0946	0.1034
Largest diff. peak and hole [e Å^{-3}]	0.95 and −0.87	1.07 and −1.47	1.02 and −1.24	2.07 and −1.44	2.28 and −2.34

Compound	**5**	**6**	**7**	**8**
Empirical formula	$C_{36}H_{36}P_2Cl_2Ta_2$	$C_{36}H_{51}O_6PCl_3Ta_3$·acetone	$C_{38}H_{59}N_4Cl_2Ta$	$C_{32}H_{52}OP_2Cl_4Ta_2$
Molecular mass	891.33	1318.01	823.74	1018.38
Temperature [K]	220(2)	220(2)	220(2)	220(2)
Crystal system	triclinic	monoclinic	monoclinic	monoclinic
Space group	$P\bar{1}$ (no. 2)	$P2_1/n$ (no. 14)	$P2_1/n$ (no. 14)	Cc (no. 9)
Unit cell dimensions				
a [Å]	9.0480(3)	11.5431(3)	15.056(2)	20.6118(1)
b [Å]	13.4376(4)	24.6455(5)	15.261(2)	16.1667(1)
c [Å]	13.9232(4)	16.1917(3)	16.911(2)	11.3250(2)
α [°]	77.837(1)	90	90	90
β [°]	75.24	105.062(1)	91.16(2)	96.195(1)
γ [°]	77.024(1)	90	90	90
V [Å^3]	1573.83(8)	4448.1(2)	3884.8(8)	3760.7(7)
Z	2	4	4	2
$\rho_{calcd.}$ [g cm^{-3}]	1.881	1.967	1.408	1.799
μ(Mo-K_α) [mm^{-1}]	7.236	7.622	2.997	6.208
F(000)	852	2524	1688	1984
$\Theta_{min.}$, Θ_{max} [°]	1.53–27.89	1.54–27.85	1.79–28.04	1.60–27.45
Index ranges				
	−11 h 11	−14 h 14	−19 h 19	−10 h 26
	−12 k 17	−32 k 30	−19 k 20	−19 k 20
	−18 l 17	−21 l 20	−22 l 22	−14 l 12
Reflections collected	8814	35789	35585	9147
Independent reflections	6373	9691	8761	4526
R(int)	0.0698	0.0472	0.0320	0.0415
Parameters	325	482	642	370
Goodness-of-fit on F^2	0.891	1.168	1.105	1.114
Final R indices [$I > 2\sigma(I)$]				
R_1	0.0473	0.0290	0.0297	0.0272
wR_2	0.1257	0.0730	0.0682	0.0696
R indices (all data)				
R_1	0.0761	0.0374	0.0372	0.0278
wR_2	0.1629	0.0848	0.0717	0.0761
Largest diff. peak and hole [e Å^{-3}]	2.02 and −1.94	0.76 and −1.86	0.57 and −0.92	1.33 and −2.13

cell of **1** contains four noninteracting diethyl ether molecules, and that of **4a** two hexane molecules.

The pronounced tendency of Ta^{IV} to form binuclear complexes is also evident in the molecular structures of **1**−**5**. The *trans* complexes **1**−**4b** are centrosymmetric dimers in which two Ta atoms are bound by two bridging phosphinidene [PCy (**1**) (Figure 1), P*t*Bu (**2**) (Figure 2), PPh (**3**) (Figure 3), PMes (Figure 4)] groups. Each Ta atom also bears a terminal chloro ligand, and a Cp* ligand completes the coordination sphere of the Ta atom (Table 3). The four-membered metallacycles Ta−P−Ta′−P′ are planar and almost square (the centres of the planar Ta_2P_2 rings in **1**−**4b** coincide with crystallographic inversion centres); this indicates substantial pπ -dπ backbonding (P→ Ta) of the phosphorus lone pair. Complex **I** exhibits comparable structural parameters.[3]

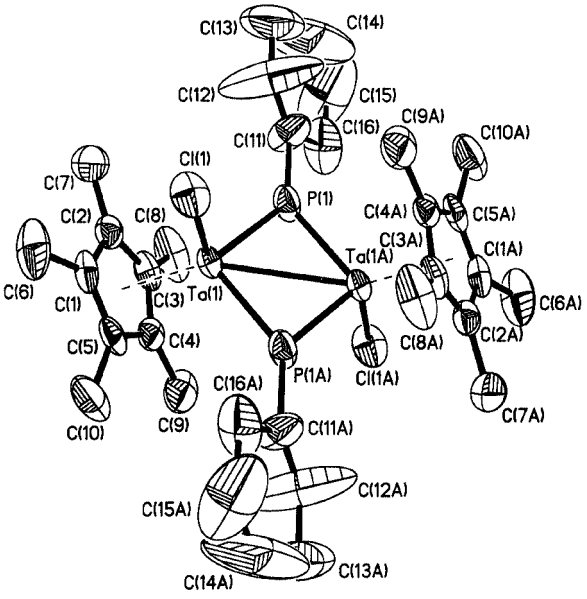

Figure 1. Molecular structure of *trans*-[{Cp*TaCl(μ-PCy)}$_2$] (**1**) showing the atom numbering scheme employed (ORTEP plot, 50% probability, SHELXTL PLUS; XP[37]). Hydrogen atoms are omitted for clarity.

In the *cis* complexes **4a** (Figure 5) and **5** (Figure 6), a butterfly-type central Ta_2P_2 ring is observed [dihedral angle for **4a**: Ta(1)−P(1)−Ta(2)/Ta(1)−P(2)−Ta(2) 27.61(6)°, **5**: Ta(1)−P(1)−Ta(2)/Ta(1)−P(2)−Ta(2) 10.4(2)°]. Due to geometric requirements, the aryl rings in **4a** are almost perpendicular to the Ta_2P planes [dihedral angles 89.9(4)° and 88.9(4)°]. This structure is also retained in solution, as indicated by two signals for the nonequivalent *meta*-H atoms (^{1}H NMR) and the *ortho*-methyl groups in the ^{1}H and ^{13}C NMR spectra. In **5**, both mesityl rings are also almost perpendicular to the Ta_2P planes [dihedral angles 86.6(4)° for P(2)-mesityl and 73.8(4)° for P(1)-mesityl]. However, in this case free rotation around the P−C_{ipso}(Mes) bond is possible in solution, as indicated by the presence of only one broad signal for the equivalent *meta*-H atoms and the *ortho*-methyl groups (^{1}H NMR).

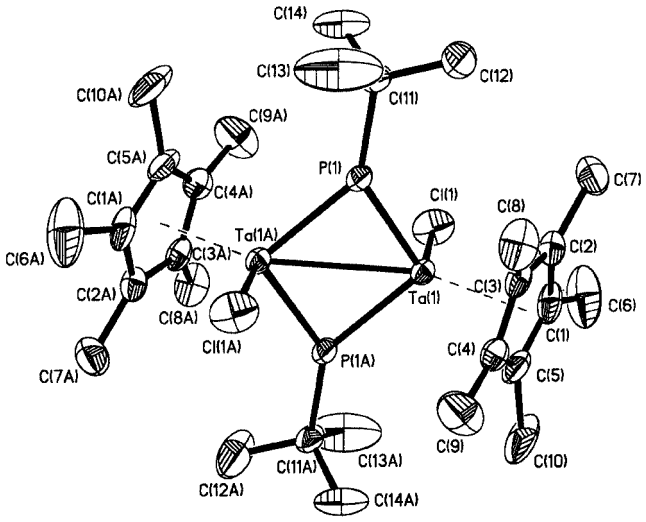

Figure 2. Molecular structure of *trans*-[{Cp*TaCl(μ-P*t*Bu)}$_2$] (**2**) showing the atom numbering scheme employed (ORTEP plot, 50% probability, SHELXTL PLUS; XP[37]). Hydrogen atoms are omitted for clarity.

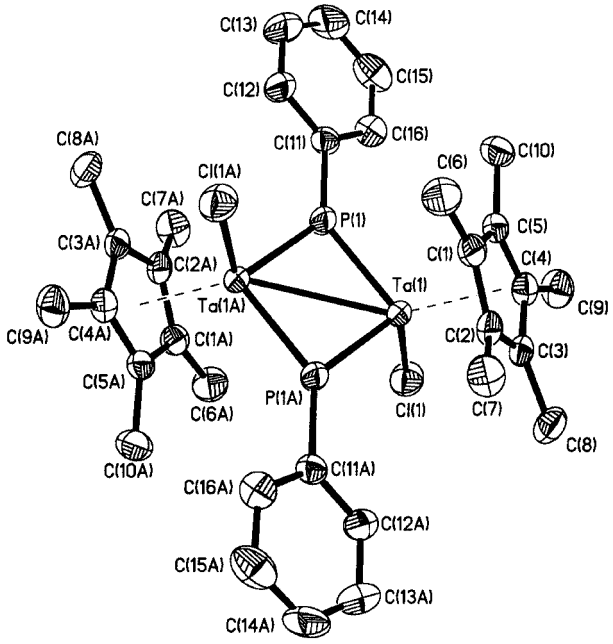

Figure 3. Molecular structure of *trans*-[{Cp*TaCl(μ-PPh)}$_2$] (**3**) showing the atom numbering scheme employed (ORTEP plot, 50% probability, SHELXTL PLUS; XP[37]). Hydrogen atoms are omitted for clarity.

Complexes **1**−**5** are diamagnetic, thus the presence of a Ta−Ta single bond can be assumed. For other dimeric complexes it was observed that the Ta−Ta bond length[19] is strongly dependent on the number and type of ligands (e.g., hydrido-bridged complexes generally have shorter Ta−Ta bonds than comparable halogen-bridged complexes[20]). A comparable value of 3.165 Å was observed for [{$TaCl_3(SMe_2)$(μ-SPh)}$_2$],[21] in which a Ta−Ta single bond is present according to theoretical calculations.[22]

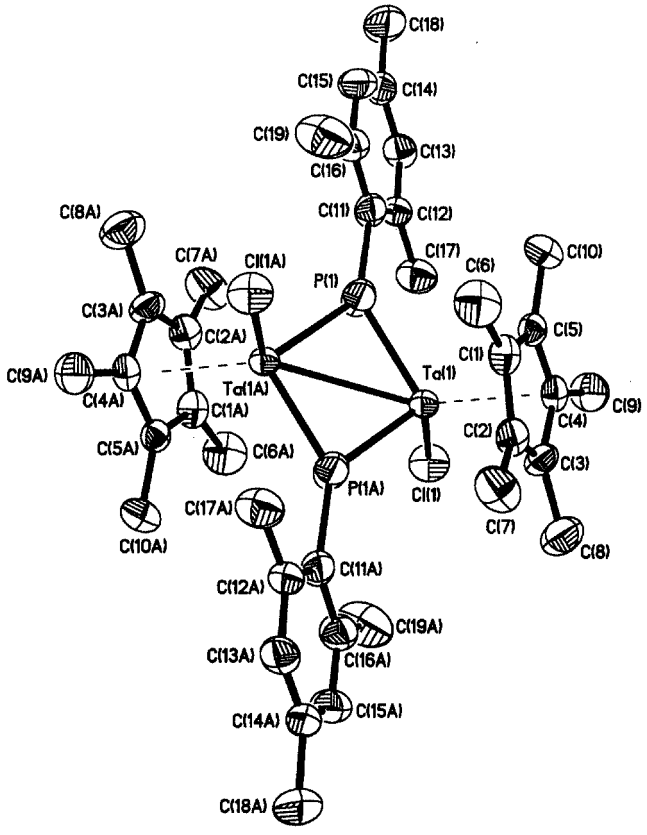

Figure 4. Molecular structure of *trans*-[{Cp*TaCl(μ-PMes)}$_2$] (**4b**) showing the atom numbering scheme employed (ORTEP plot, 50% probability, SHELXTL PLUS; XP[37]). Hydrogen atoms are omitted for clarity.

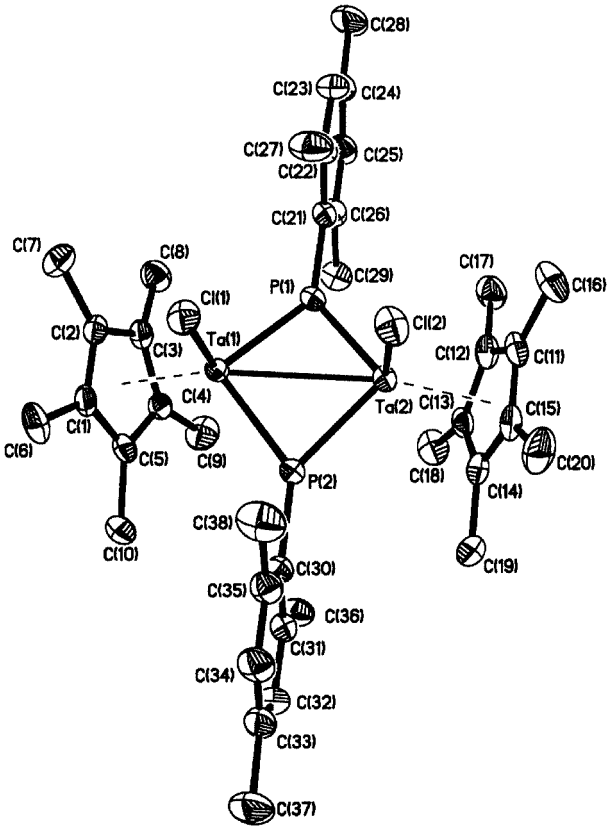

Figure 5. Molecular structure of *cis*-[{Cp*TaCl(μ-PMes)}$_2$] (**4a**) showing the atom numbering scheme employed (ORTEP plot, 50% probability, SHELXTL PLUS; XP[37]). Hydrogen atoms are omitted for clarity.

Table 3. Selected bond lengths [Å] and angles [°] of compounds **1**–**5** and [(Cp′TaCl{μ-P(Tipp)})$_2$] (**I**)[3]

Compound	Ta–P	Ta–Ta	Ta–Cl	Ta–P–Ta	P–Ta–P
1	2.334(2), 2.336(2)	3.132(1)	2.358(2)	84.26(6)	95.74(6)
2	2.354(1), 2.357(1)	3.1759(8)	2.360(1)	84.78(4)	95.22(4)
3	2.345(1), 2.344(1)	3.1957(6)	2.357(1)	85.92(4)	94.08(4)
4a	3 × 2.344(2), 2.349(1)	3.0881(3)	2.347(2), 2.352(2)	82.31(5), 82.39(5)	93.87(5), 94.00(5)
4b	2.328(2), 2.331(2)	3.0773(5)	2.364(2)	82.68(7)	97.32(7)
5	2.348(3), 2.358(3) 2.336(3), 2.357(3)	3.1253(7)	2.351(3), 2.365(3)	83.0(1), 83.7(1)	95.9(1), 96.3(1)
I	2.317(6), 2.338(2)	3.100(3)	2.350(2)	83.51(8)	96.49(8)

The Ta–P bond lengths in **1**–**5** are similar to those of **I**[3] (Table 3) and the terminal phosphinidene complex [(*t*Bu$_3$SiO)$_3$Ta=PPh][5] [2.317(4) Å] with a bent TaPC arrangement [Ta–P–C 110.2(4)°], while [N{CH$_2$CH$_2$N(SiMe$_3$)}$_3$Ta=PCy][6] has a linear TaPC arrangement and a shorter Ta–P bond of 2.145(7) Å. However, all these distances are shorter than the sum of the covalent radii of Ta and P (2.44 Å).[23] Longer bonds are observed for bridging phosphanido ligands (e.g., [{Cp′Ta(PPh$_2$)(μ-PPh$_2$)}$_2$], Ta–P$_{br}$ 2.486(2), 2.458(2) Å].[3]

The trigonal-planar geometry of the P atoms of the bridging phosphinidene group in the *trans* complexes **1**–**4b** (sum of bond angles ca. 360°) indicates that the PR group acts as a three-electron donor. In the *cis* complexes **4a** and **5**, the P atoms also have a trigonal-planar environment [sum of bond angles **4a**: P(1): 358.0(2)°, P(2): 357.8(2)°, **5**: P(1): 356.8(4)°, P(2): 358.8(4)°].

The Ta–Cl bonds in **1**–**5** (Table 3) are shorter than those in the Ta chloro phosphane complexes (e.g., [{TaCl$_2$(μ-Cl)(μ-PMe$_2$CH$_2$PMe$_2$)}$_2$], Ta–Cl (terminal) 2.435(7), 2.457(6) Å;[24] *trans*-[CpTaCl$_2$(CO)(PMe$_2$Ph)$_2$], Ta–Cl 2.518(4), 2.539(4) Å;[25] [Cp*TaCl$_3$(PMe$_3$)], Ta–Cl 2.395(3) to 2.416(3) Å;[26] *cis*-[Cp*TaCl$_2$(CO)$_2$(PMe$_3$)], Ta–Cl 2.504(2), 2.512(2) Å[26]).

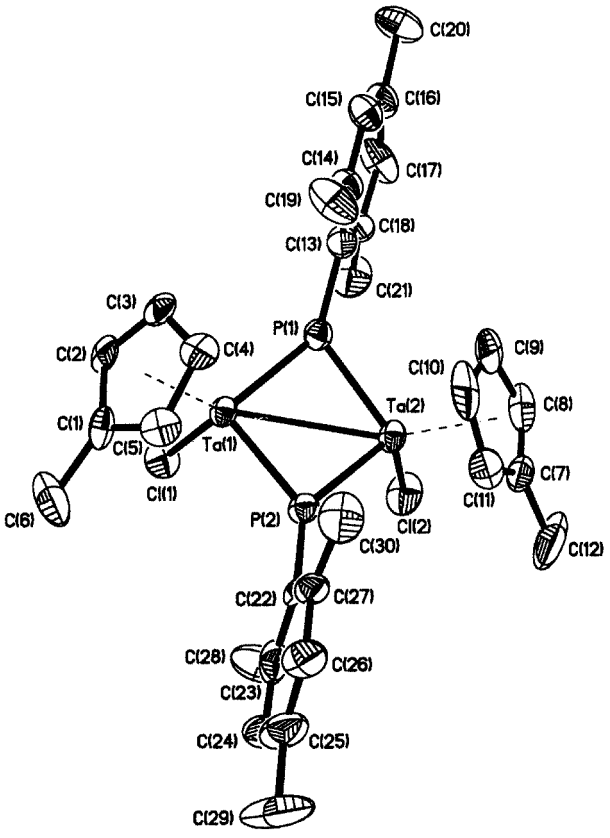

Figure 6. Molecular structure of *cis*-[{Cp′TaCl(μ-PMes)}$_2$] (**5**) showing the atom numbering scheme employed (ORTEP plot, 50% probability, SHELXTL PLUS; XP[37]). Hydrogen atoms are omitted for clarity.

Reactivity of 1, 3 and 4

While terminal electrophilic phosphinidene complexes are highly reactive,[27] **1**−**5** are air-stable as solids for at least several hours. **1**, **3** and **4b** also exhibit a remarkable stability towards acetone, benzophenone, acetonitrile, CS_2 (**1** and **3**), acetaldehyde (**4b**), or $EtAlCl_2$ (**3**), even at elevated temperatures.

Complex **3** reacts with moist acetone (50-fold excess) in the presence of traces of air to give the trinuclear cluster [{Cp*TaCl(μ$_2$-O)}$_3$(μ$_3$-O)(μ-O$_2$PHPh)}] (**6**) in very low yield (Scheme 2). **6** was only characterised by crystal structure determination.

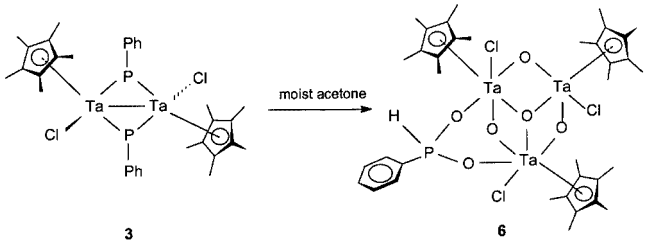

3 6

Scheme 2

Complex **6** crystallises as yellow prismatic crystals in the monoclinic space group $P2_1/n$ with four molecules of acetone in the unit cell. The central structural fragment is a Ta_3O_4 cluster, in which the Ta^V and O atoms alternatingly occupy the corners of a heterocubane with one missing corner (Figure 7). Related clusters have been reported for Zr, Nb, Ta and Mo.[28] Each Ta atom is coordinated by a Cp* and one terminal chloro ligand. Two Ta atoms have a coordination number of six [Ta(1) and Ta(2)]; Ta(3) is five-coordinate. The Ta−Ta distances range from 3.1185(3) to 3.3378(3) Å. There are two types of O atoms: one triply-bridging [O(6)] and three doubly-bridging oxo ligands [O(3), O(4), and O(5); Ta−O 1.910(3) to 2.003(3) Å]. The latter Ta−O bond lengths are in the range for single bonds,[28a,28b] while the Ta−O(6) bond lengths differ by

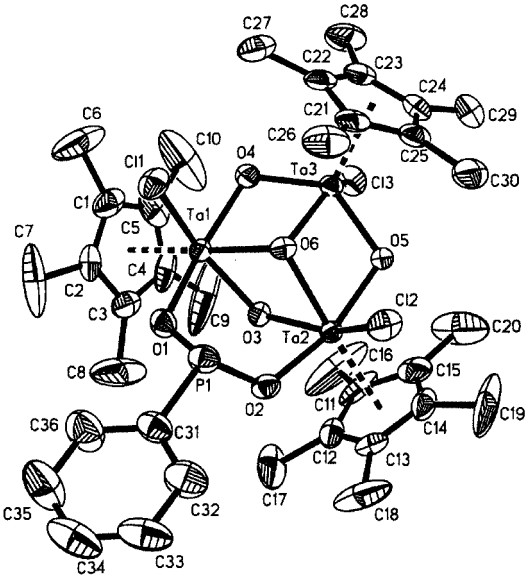

Figure 7. Molecular structure of [{Cp*TaCl(μ$_2$-O)}$_3$(μ$_3$-O)(μ$_2$-O$_2$PHPh)}] (**6**) showing the atom numbering scheme employed (ORTEP plot, 50% probability, SHELXTL PLUS; XP[37]). Hydrogen atoms are omitted for clarity. Bond lengths [Å] and angles [°]: Ta(1)−O(4) 1.960(3), Ta(1)−O(3) 1.991(3), Ta(1)−O(1) 2.127(3), Ta(1)−O(6) 2.148(3), Ta(2)−O(5) 1.964(3), Ta(2)−O(3) 2.003(3), Ta(2)−O(2) 2.117(3), Ta(2)−O(6) 2.136(3), Ta(3)−O(5) 1.910(3), Ta(3)−O(4) 1.915(3), Ta(3)−O(6) 2.058(3), Ta(1)−Cl(1) 2.506(1), Ta(2)−Cl(2) 2.491(1), Ta(3)−Cl(3) 2.429(1), Ta(1)−Ta(3) 3.1185(3), Ta(1)−Ta(2) 3.3378(3), Ta(2)−Ta(3) 3.1206(3), P(1)−O(1) 1.510(4), P(1)−O(2) 1.514(4), P(1)−C(31) 1.778(6); O(4)−Ta(1)−O(3) 98.6(1), O(4)−Ta(1)−O(1) 155.9(1), O(3)−Ta(1)−O(1) 86.6(1), O(4)−Ta(1)−O(6) 74.0(1), O(3)−Ta(1)−O(6) 71.2(1), O(1)−Ta(1)−O(6) 85.7(1), O(4)−Ta(1)−Cl(1) 86.9(1), O(3)−Ta(1)−Cl(1) 148.8(1), O(1)−Ta(1)−Cl(1) 77.1(1), O(6)−Ta(1)−Cl(1) 81.05(9), O(5)−Ta(2)−O(3) 97.7(1), O(5)−Ta(2)−O(2) 156.1(1), O(3)−Ta(2)−O(2) 86.2(1), O(5)−Ta(2)−O(6) 74.0(1), O(3)−Ta(2)−O(6) 71.2(1), O(2)−Ta(2)−O(6) 85.1(1), O(5)−Ta(2)−Cl(2) 87.6(1), O(3)−Ta(2)−Cl(2) 148.7(1), O(2)−Ta(2)−Cl(2) 77.5(1), O(6)−Ta(2)−Cl(2) 80.91(9), O(5)−Ta(3)−O(6) 76.9(1), O(4)−Ta(3)−O(6) 77.0(1), O(5)−Ta(3)−Cl(3) 86.0(1), O(4)−Ta(3)−Cl(3) 85.4(1), O(6)−Ta(3)−Cl(3) 136.68(9), O(1)−P(1)−O(2) 112.5(2), O(1)−P(1)−C(31) 109.4(3), O(2)−P(1)−C(31) 109.2(2), P(1)−O(1)−Ta(1) 123.7(2), P(1)−O(2)−Ta(2) 124.8(2), Ta(1)−O(3)−Ta(2) 113.4(2), Ta(3)−O(4)−Ta(1) 107.2(2), Ta(3)−O(5)−Ta(2) 107.3(2), Ta(3)−O(6)−Ta(2) 96.1(1), Ta(3)−O(6)−Ta(1) 95.7(1), Ta(2)−O(6)−Ta(1) 102.4(1), C(36)−C(31)−P(1) 122.1(5), C(32)−C(31)−P(1) 120.0(5).

ca. 0.1 Å [Ta(3)−O(6) 2.058(3), Ta(1)−O(6) 2.148(3), Ta(2)−O(6) 2.136(3) Å]. For Ta(1) and Ta(2), the *trans* effect of the Cp* ligand apparently affects the Ta−O bond lengths. Similar structural data were found for [(Cp*TaCl)$_3$(μ_2-Cl)(μ_2−O)$_2$(μ_3-O)(μ-O$_2$Si*t*Bu$_2$)].[28b]

In addition, a P(H)(Ph)O$_2^-$ ligand, the anion of phenyl phosphinic acid, bridges Ta(1) and Ta(2). However, the PH proton could not be localised. Due to the small amount of **6** available, no ^{31}P NMR spectrum could be obtained to verify the presence of the PH proton. However, since tantalum(v) is present in this cluster, the presence of an anionic P(H)(Ph)O$_2^-$ ligand must be assumed. The P−O bond lengths indicate multiple bond character (ca. 1.51 Å).[28f]

While no reaction of **3** with one or two equivalents of CyNC was observed, a 10-fold excess of CyNC gave the tantalum(III) complex [Cp*TaCl(CNCy)$_4$]Cl (**7**) (Scheme 3), which was characterised by ^{1}H, ^{13}C NMR spectroscopy and

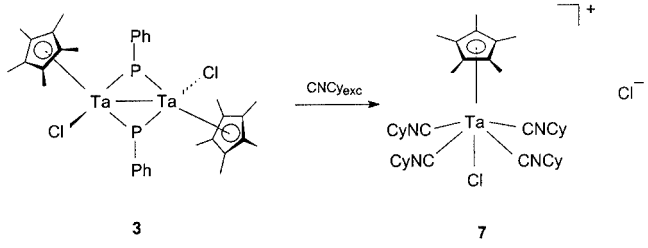

Scheme 3

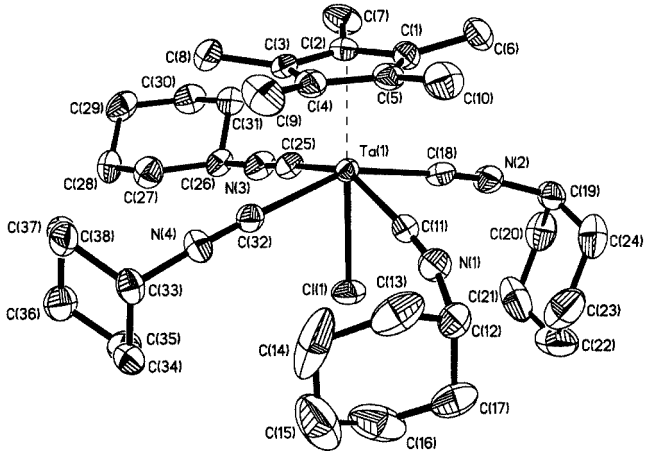

Figure 8. Molecular structure of [Cp*TaCl(CNCy)$_4$]Cl (**7**) showing the atom numbering scheme employed (ORTEP plot, 50% probability, SHELXTL PLUS; XP[37]). Only the cation is shown. Hydrogen atoms are omitted for clarity; selected bond lengths [Å] and angles [°]: Ta(1)−C(11) 2.179(4), Ta(1)−C(32) 2.185(4), Ta(1)−C(18) 2.187(4), Ta(1)−C(25) 2.187(4), Ta(1)−Cl(1) 2.5146(9), N(1)−C(11) 1.151(5), N(1)−C(12) 1.460(5), N(2)−C(18) 1.147(5), N(2)−C(19) 1.452(5), N(3)−C(25) 1.154(5), N(3)−C(26) 1.452(5), N(4)−C(32) 1.152(5), N(4)−C(33) 1.459(5); C(11)−Ta(1)−C(32) 84.69(13), C(11)−Ta(1)−C(18) 87.54(14), C(32)−Ta(1)−C(18) 153.37(13), C(11)−Ta(1)−C(25) 153.23(13), C(32)−Ta(1)−C(25) 86.15(13), C(18)−Ta(1)−C(25) 89.51(14), C(11)−Ta(1)−Cl(1) 76.99(10), C(32)−Ta(1)−Cl(1) 76.98(10), C(18)−Ta(1)−Cl(1) 76.46(10), C(25)−Ta(1)−Cl(1) 76.45(10), C(11)−N(1)−C(12) 165.6(4), C(18)−N(2)−C(19) 166.5(4), C(25)−N(3)−C(26) 174.6(4), C(32)−N(4)−C(33) 175.5(4), N(1)−C(11)−Ta(1) 176.1(3), N(2)−C(18)−Ta(1) 176.0(3), N(3)−C(25)−Ta(1) 177.2(3), N(4)−C(32)−Ta(1) 177.7(3).

by crystal structure determination. A molecular ion peak was observed for the cation in **7** by FAB-MS (3-nitrobenzaldehyde as matrix) at m/z = 786. In the ^{31}P NMR spectrum of the reaction mixture, signals for the oxidation products (PPh)$_n$ (n = 4−6)[29] were observed. In addition, two doublets (δ = −57.8 ppm and −121.4 ppm, $^1J_{PP}$ = 311 Hz) were observed, which we could not assign.

Complex **7** crystallises as orange rhombic crystals from THF in the monoclinic space group $P2_1/n$. In the cation (Figure 8), the NC group occupies the axial position in three of the four cyclohexyl groups of the isocyanide ligands. The reason for this unexpected arrangement is the formation of hydrogen bonds between the hydrogen atom of the α-C atom C(26) of the isocyanide ligand in which the NC group is in the equatorial position and the hydrogen atom on the β-C atom of an isocyanide ligand of a second molecule to a chloride anion (Figure 9). However, in solution the four isocyanide ligands are equivalent (^{13}C NMR).

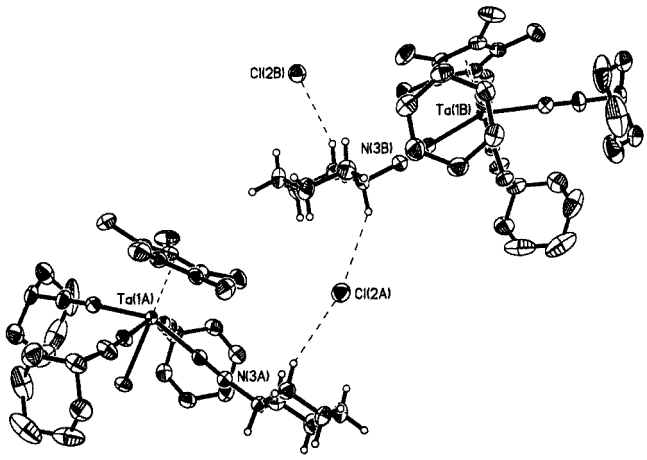

Figure 9. Hydrogen bonding in [Cp*TaCl(CNCy)$_4$]Cl (**7**) (ORTEP plot, 50% probability, SHELXTL PLUS; XP[37]).

For the TaCN group, two mesomeric structures can be formulated (as for carbonyl groups):

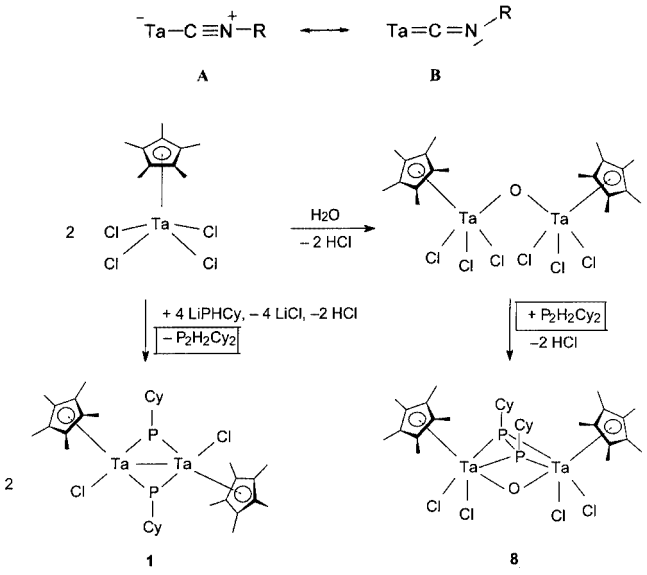

Scheme 4

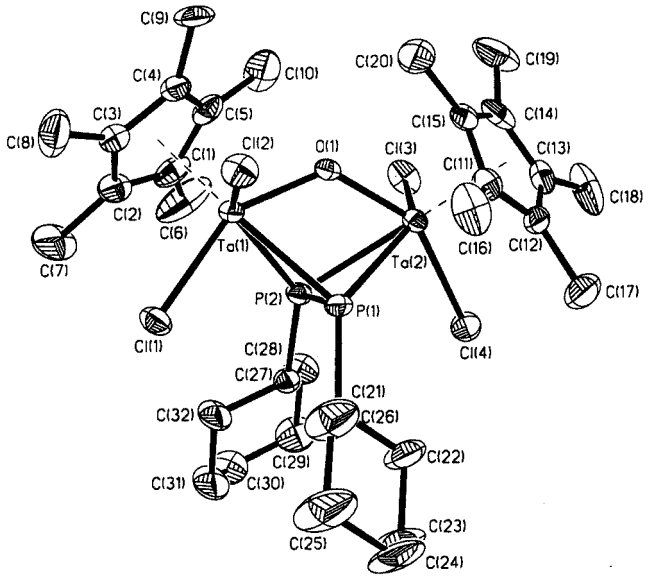

Figure 10. Molecular structure of $[(Cp^*TaCl_2)_2(\mu_2\text{-}O)(\eta^2,\mu_2\text{-}P_2Cy_2)]$ (**8**) showing the atom numbering scheme employed (ORTEP plot, 50% probability, SHELXTL PLUS; XP[37]). Hydrogen atoms are omitted for clarity. Bond lengths [Å] and angles [°]: Ta(2)−O(1) 1.974(6), Ta(2)−Cl(3) 2.413(2), Ta(2)−Cl(4) 2.425(2), Ta(2)−P(1) 2.580(2), Ta(2)−P(2) 2.600(2), Ta(1)−O(1) 1.978(6), Ta(1)−Cl(2) 2.407(2), Ta(1)−Cl(1) 2.413(2), Ta(1)−P(2) 2.578(2), Ta(1)−P(1) 2.602(2), P(1)−C(21) 1.884(9), P(1)−P(2) 2.188(3), P(2)−C(27) 1.864(9); O(1)−Ta(2)−Cl(3) 94.31(18), O(1)−Ta(2)−Cl(4) 148.73(17), Cl(3)−Ta(2)−Cl(4) 88.86(9), O(1)−Ta(2)−P(1) 69.02(17), Cl(3)−Ta(2)−P(1) 137.96(8), Cl(4)−Ta(2)−P(1) 88.01(8), O(1)−Ta(2)−P(2) 67.73(17), Cl(3)−Ta(2)−P(2) 88.14(8), Cl(4)−Ta(2)−P(2) 81.33(8), P(1)−Ta(2)−P(2) 49.97(8), O(1)−Ta(1)−Cl(2) 94.81(17), O(1)−Ta(1)−Cl(1) 148.85(16), Cl(2)−Ta(1)−Cl(1) 90.28(8), O(1)−Ta(1)−P(2) 68.17(17), Cl(2)−Ta(1)−P(2) 137.60(8), Cl(1)−Ta(1)−P(2) 87.57(7), O(1)−Ta(1)−P(1) 68.49(16), Cl(2)−Ta(1)−P(1) 87.88(8), Cl(1)−Ta(1)−P(1) 81.04(8), P(2)−Ta(1)−P(1) 49.97(8), C(21)−P(1)−P(2) 111.3(4), C(21)−P(1)−Ta(2) 138.1(3), P(2)−P(1)−Ta(2) 65.49(9), C(21)−P(1)−Ta(1) 131.2(3), P(2)−P(1)−Ta(1) 64.45(9), Ta(2)−P(1)−Ta(1) 87.02(7), C(27)−P(2)−P(1) 111.2(3), C(27)−P(2)−Ta(1) 138.2(3), P(1)−P(2)−Ta(1) 65.57(9), C(27)−P(2)−Ta(2) 131.0(3), P(1)−P(2)−Ta(2) 64.55(9), Ta(1)−P(2)−Ta(2) 87.10(7), Ta(2)−O(1)−Ta(1) 129.1(3).

As the Ta−C bond lengths of the isocyanide ligands [2.179(4) to 2.187(4) Å] are in the range of Ta−C single bonds and the C−N−C(Cy) groups are almost linear [165.6(4)° to 175.5(4)°], mesomeric structure **A** can be assumed. The Ta atom is located 0.502(2) Å above the plane of the four isocyanide carbon atoms.

As a minor product, $[(Cp^*TaCl_2)_2(\mu_2\text{-}O)(\eta^2,\mu_2\text{-}P_2Cy_2)]$ (**8**) was also obtained in the reaction of $[Cp^*TaCl_4]$ with one equivalent of LiPHCy. **8** was only characterised by crystal structure determination; in the ^{31}P NMR spectrum of the reaction mixture a singlet of low intensity at $\delta = 538.6$ ppm was observed, which could be attributed to **8** or a precursor complex thereof. As two doublets are observed in the high-field region of the ^{31}P NMR spectrum of $[Cp_2TaH(\eta^2\text{-}P_2R_2)]$ (R = Ph:[2a,30] $\delta = -145.1$ ppm and -162.8 ppm, R = Cy:[30] $\delta = -123.1$ ppm and -143.3 ppm) the latter seems more likely.

A possible route for the formation of **8** is hydrolysis of $[Cp^*TaCl_4]$ to give $[(Cp^*TaCl_3)_2(\mu\text{-}O)]$, which can then react with $P_2H_2R_2$ (formed in the redox reaction which gives **1**) to yield the observed product (Scheme 4).

Complex **8** crystallises in the monoclinic space group *Cc*. In **8**, two Cp^*TaCl_2 fragments are bridged by one oxo ligand and a diphosphanediyl group $P_2Cy_2^{2-}$; this indicates the presence of Ta^V (Figure 10). In general, free diphosphenes P_2R_2 are only stable when sterically demanding R groups are present;[31] however, unstable derivatives can be stabilised by coordination to a transition metal.[32] The Ta−P bond lengths [Ta(2)−P(1) 2.580(2), Ta(2)−P(2) 2.600(2), Ta(1)−P(2) 2.578(2), Ta(1)−P(1) 2.602(2) Å] are in the range observed for other tantalum diphosphene complexes [2.602(5) to 2.632(5) Å].[32]

In **8**, the P(1)−P(2) bond length of 2.188(3) Å indicates a single bond. In the tantalum diphosphene complexes $[Cp_2TaH(\eta^2\text{-}P_2R_2)]$ (R = Cy, H) the P−P bond lengths are shorter [2.131(3) and 2.136(6) Å].[30]

Experimental Section

All experiments were carried out under purified dry argon. Solvents were dried and freshly distilled under argon. The NMR spectra were recorded with an AVANCE DRX 400 spectrometer (Bruker), ^1H NMR: internal standard solvent (benzene or $CDCl_3$), external standard $SiMe_4$. ^{13}C NMR: external standard $SiMe_4$, internal standard solvent. ^{31}P NMR: external standard 85% H_3PO_4. The IR spectra were recorded with a FT-IR spectrometer Perkin−Elmer System 2000 in the range 350−4000 cm^{-1}. UV/Vis spectra were recorded in pentane with a LAMBDA 900 (Perkin−Elmer) in an inert-gas cuvette. The melting points were determined in sealed capillaries under argon and are uncorrected. LiPHCy,[11] LiPH*t*Bu,[12] LiPHPh,[13] LiPHMes,[14] [Cp′$TaCl_4$][16] and $[Cp^*TaCl_4]$[10] were prepared by literature procedures.

General Procedure for the Preparation of *trans*-[{Cp*TaCl(μ-PR)}$_2$] [R = Cy (1), *t*Bu (2), Ph (3), Mes (4b)]: A suspension of $[Cp^*TaCl_4]$ in toluene (30 mL) was cooled to −70 °C, and two equivalents of LiPHR were added to the stirred reaction mixture over 2 h. The resulting suspension was slowly warmed to room temperature and stirred overnight. The solvent was removed and the solid dissolved in diethyl ether (**1**, **3**), pentane (**2**), or hexane (**4b**). The mixture was filtered. Deep red crystals were obtained by cooling the filtrate to 5 °C.

The Ta^{IV} phosphinidene complex (Table 1) and the oxidation products $P_2H_2R_2$ (or their decomposition products: cyclic oligophosphanes and the free phosphane RPH_2) were detected by ^{31}P NMR spectroscopy. The following signals were observed for the oxidation products:

*t*Bu: $\delta = -57.5$ ppm [s, $(PtBu)_4$],[29] −71.7 (d) and −108.0 (t) $(PtBu)_3$ ppm.[33]

Cy: $\delta = -68.3$ (s, $PCy)_4$, −84.3 and −87.5 (m, *rac*- and *meso*-$P_2H_2Cy_2$),[29] −111.0 (t, PH_2Cy) ppm.

Ph: δ = ca. 3 [m, $(PPh)_5$], −21.3 [s, $(PPh)_6$], −47.6 [s, $(PPh)_4$][29,34] −67.4, −70.9 (m, *meso*- and *rac*-$P_2H_2Ph_2$; the signal for the unstable diphosphane disappears after two days),[35,36] −122.1 (t, PH_2Ph) ppm.

Mes: $\delta = -43.2$ [s, $(PMes)_4$], −109.3 (d), −143.9 (t) $(PMes)_3$, −110.4, −117.5 (m, *meso*- and *rac*-$P_2H_2Mes_2$), −153.8 (t, PH_2Mes) ppm.

1: (0.45 g, 0.98 mmol) [Cp*$TaCl_4$], (0.48 g, 1.96 mmol) LiPHCy, rhombohedral deep red crystals of **1**·2 Et_2O, yield: 0.40 g (81% rel. [Cp*$TaCl_4$]), m.p. 319 °C (dec.). ^{1}H NMR (400 MHz, C_6D_6, 25 °C): δ = 1.12 [t, $^3J_{H,H}$ = 7.0 Hz, 6 H, CH_3 in ether], 1.38 (m, 4 H, 4-H in Cy), 1.46 (m, 8 H, 3-H/5-H in Cy), 1.76 (m, 8 H, 2-H/6-H in Cy), 2.00 (m, 2 H, 1-H in Cy), 2.20 (s, 30 H, CH_3 in Cp*), 3.27 [q, $^3J_{H,H}$ = 7.0 Hz, 4 H, CH_2 in ether] ppm. ^{13}C{^{1}H} NMR (100.61 MHz, C_6D_6, 25 °C): δ = 14.0 (*C*H_3 in C_5Me_5), 16.2 (*C*H_3 in ether), 27.5 (C-4 in Cy), 30.0 [d, $^3J_{P,C}$ = 19 Hz; C-3/C-5 in Cy], 35.9 [d, $^2J_{P,C}$ = 79 Hz; C-2/C-6 in Cy], 52.1 (br; C-1 in Cy), 66.6 (*C*H_2 in ether), 114.9 (*C*$_5$Me$_5$) ppm. Solvent-free **1**, $C_{32}H_{52}Cl_2P_2Ta_2$ (931.51): C 41.3, H 5.6, Cl 7.6; found C 40.4, H 5.3, Cl 7.2.

2: (0.40 g, 0.87 mmol) [Cp*$TaCl_4$], (0.17 g, 1.77 mmol) LiPH*t*Bu, yield: 0.33 g (86% rel. [Cp*$TaCl_4$]), m.p. 341 °C (dec.), prismatic deep red crystals. ^{1}H NMR (400 MHz, C_6D_6, 25 °C): δ = 1.48 [d, $^3J_{P,H}$ = 14 Hz, 18 H, *t*Bu], 2.18 (s, 30 H, CH_3 in Cp*) ppm. ^{13}C{^{1}H} NMR (100.61 MHz, C_6D_6, 25 °C): δ = 14.8 (*C*H_3 in C_5Me_5), 35.1 [C(*C*H_3)$_3$], 35.6 [*C*(CH$_3$)$_3$], 116.4 (*C*$_5$Me$_5$) ppm. $C_{28}H_{48}Cl_2P_2Ta_2$ (879.40): calcd. C 38.3, H 5.5, Cl 8.1; found C 38.8, H 5.6, Cl 8.1.

3: (0.50 g, 1.09 mmol) [Cp*$TaCl_4$], (0.25 g, 2.20 mmol) LiPHPh, yield: 0.42 g (85% rel. [Cp*$TaCl_4$]), m.p. 341 °C (dec.), rhombohedral deep red crystals. ^{1}H NMR (400 MHz, C_6D_6, 25 °C): δ = 2.03 (s, 30 H, CH_3 in Cp*), 6.97 (br, 2 H, *p*-H in Ph), 7.36 [pseudo t, $^3J_{H,H}$ = 14, $^3J_{P,H}$ = 14 Hz, 4 H, *o*-H in Ph], 8.17 [t, $^3J_{H,H}$ = 14 Hz, 4 H, *m*-H in Ph] ppm. ^{13}C{^{1}H} NMR (100.61 MHz, C_6D_6, 25 °C): δ = 13.6 (*C*H_3 in C_5Me_5), 115.3 (*C*$_5$Me$_5$), 129.7 (*p*-C in Ph), 125.2 (*m*-C in Ph), 136.0 (*o*-C in Ph), 148.6 (*ipso*-C in Ph) ppm. $C_{32}H_{40}Cl_2P_2Ta_2$ (919.38): calcd. Cl 7.7; found Cl 8.1.

4b: (0.40 g, 0.87 mmol) [Cp*$TaCl_4$], (0.28 g, 1.8 mmol) LiPHMes, yield: 0.32 g (73% rel. [Cp*$TaCl_4$]), m.p. 321 °C (dec.), rhombohedral deep red crystals. ^{1}H NMR (400 MHz, C_6D_6, 25 °C): δ = 2.01 (s, 30 H, CH_3 in Cp*), 2.22 (s, 6 H, *p*-Me in Mes), 2.72 (s, 12 H, *o*-Me in Mes), 7.01 (s, 4 H, *m*-H in Mes) ppm. ^{13}C{^{1}H} NMR (100.61 MHz, C_6D_6, 25 °C): δ = 13.3 (*C*H_3 in C_5Me_5), 22.0 (*p*-Me in Mes), 25.9 (*o*-Me in Mes), 115.2 (*C*$_5$Me$_5$), 130.5 (*m*-C in Mes), 132.9 (*p*-C in Mes), 139.4 (*o*-C in Mes), 144.8 (*ipso*-C in Mes) ppm. $C_{38}H_{52}Cl_2P_2Ta_2$ (1003.54): calcd. C 45.5, H 5.2; Cl 7.1; found C 45.9, H 5.4, Cl 7.0.

Synthesis of *cis*-[{Cp*TaCl(μ-PMes)}$_2$] (4a): A suspension of one equivalent of [Cp*$TaCl_4$] (0.5 g, 1.09 mmol) in toluene (30 mL) was cooled to −70 °C, and one equivalent of LiPHMes (0.17 g, 1.09 mmol) was added to the stirred reaction mixture over 3 h. The resulting suspension was stirred at −70 °C for 2 h, and then slowly warmed to room temperature and stirred overnight. The solvent was removed under vacuum, and the solid recrystallised twice from *n*-hexane. Yield: 80 mg (29% rel. LiPHMes); m.p. 289 °C (dec.). ^{1}H NMR (400 MHz, C_6D_6, 25 °C): δ = 2.05 (s, 30 H, CH_3 in Cp*), 2.26 (s, 6 H, *p*-Me in Mes), 2.39 (s, 6 H, *o*-Me in Mes), 2.56 (s, 6 H, *o*-Me in Mes), 6.91 (s, 2 H, *m*-H in Mes), 6.97 (s, 2 H, *m*-H in Mes) ppm. ^{13}C{^{1}H} NMR (100.61 MHz, C_6D_6, 25 °C): δ = 12.9 (*C*H_3 in C_5Me_5), 21.8 (*p*-Me in Mes), 23.1 (*o*-Me in Mes), 24.3 (*o*-Me in Mes), 115.5 (*C*$_5$Me$_5$), 128.0 (*m*-C in Mes), 130.9 (*m*-C in Mes),139.7 (*p*-C in Mes), 142.1 (*o*-C in Mes), 145.7 (*o*-C in Mes), 149.3 (*ipso*-C in Mes) ppm. $C_{38}H_{52}Cl_2P_2Ta_2$ (1003.54): calcd. C 45.5, H 5.2; Cl 7.1; found C 45.8, H 6.0, Cl 6.8.

Synthesis of *cis*-[{Cp′TaCl(μ-PMes)}$_2$] (5): A suspension of [Cp′$TaCl_4$] (0.4 g, 0.99 mmol) in toluene (20 mL) was cooled to −70 °C, and one equivalent of LiPHMes (0.15 g, 0.98 mmol) was added to the stirred reaction mixture over 3 h. The resulting suspension was stirred at −70 °C for 2 h, and then slowly warmed to room temperature and stirred overnight. The solvent was removed in vacuo, and the solid recrystallised twice from *n*-hexane. Yield: 0.19 g (43.5% rel. LiPHMes), rhombohedral orange-red crystals; m.p. 276 °C (dec.). ^{1}H NMR (400 MHz, C_6D_6, 25 °C): δ = 2.00 (s, 6 H, C_5MeH_4), 2.34 (s, 6 H, *p*-Me in Mes), 2.49 (br, 12 H, *o*-Me in Mes), 5.72 (t, $J_{H,H}$ = 2.6 Hz, 4 H, C_5MeH_4), 6.27 (t, $J_{H,H}$ = 2.6 Hz, 4 H, C_5MeH_4), 6.64 (br, 4 H, *m*-H in Mes) ppm. $C_{30}H_{36}Cl_2P_2Ta_2$ (891.33): C 40.4, H 4.1, Cl 8.0; found C 40.6, H 4.2, Cl 7.7.

Synthesis of [Cp*TaCl(CNCy)$_4$]Cl (7): Cyclohexyl isocyanide (0.17 g, 1.6 mmol) was added to a solution of **3** (0.15 g, 0.16 mmol) in toluene (20 mL). Over 3 days, the red solution turned orange. The solvent was removed under vacuum, and the solid recrystallised from THF to give **7** as rhombic orange crystals (0.10 g, 38% rel. to **3**); m.p. 345 °C (dec.). ^{1}H NMR (400 MHz, $CDCl_3$, 25 °C): δ = ca. 1.3 (m, 24 H, 3-H, 4-H, 5-H in Cy), ca. 1.7 (m, 16 H, 2-H, 6-H in Cy), 2.29 (s, 15 H, CH_3 in Cp*), 4.45 (br, 4 H, 1-H in Cy) ppm. ^{13}C{^{1}H} NMR (100.61 MHz, $CDCl_3$, 25 °C): δ = 13.7 (*C*H_3 in C_5Me_5), 23.5 (C-4 in Cy), 26.1 (C-3 and C-5 in Cy), 33.5 (C-2 and C-6 in Cy), 55.4 (C-1 in Cy), 70.3 (*C*NCy) 102.2 (*C*$_5$Me$_5$) ppm. $C_{38}H_{59}Cl_2N_4Ta$ (823.74): C 55.4, H 7.2, Cl 8.6; found C 55.0, H 7.8, Cl 8.4.

Data Collection and Structural Refinement of 1−8: Details of the data collection and crystal structure refinement are summarised in Table 2. Data (Mo-*Kα* , λ = 0.71073 Å) were collected with a Siemens CCD (SMART). All observed reflections were used for determination of the unit cell parameters. The structures were solved by direct methods (SHELXTL PLUS[37]) and subsequent difference Fourier syntheses and refined by full-matrix least-squares on F^2 (SHELXTL PLUS[37]). Restrictions for **1−8**: Ta, Cl, C, O, N and P atoms anisotropic, H atoms located or in calculated positions and refined isotropically. Absorption correction with SADABS[38]. CCDC-181631 (**1**), −181629 (**2**), −181627 (**3**),- 181633 (**4a**), −181635 (**4b**), −181632 (**5**), −181630 (**6**), −181628 (**7**) and CCDC-181634 (**8**) contain the supplementary crystallographic data for this paper. These data can be obtained free of charge at www.ccdc.cam.ac.uk/conts/retrieving.html [or from the Cambridge Crystallographic Data Centre, 12, Union Road, Cambridge CB2 1EZ, UK; Fax: (internat.) +44-1223/336-033; E-mail: deposit@ccdc.cam.ac.uk].

Acknowledgments

We gratefully acknowledge support of this work by the Landesgraduiertenförderung Sachsen (scholarship for S. B.). We thank the company H. C. Starck GmbH & Co. KG for a generous donation of $TaCl_5$.

[1] Eds. E. W. Abel, F. G. A. Stone, G. Wilkinson, *Comprehensive Organometallic Chemistry II*, Volumes 4 and 5, Pergamon Press, **1995**.

[2] [2a] J. C. Leblanc, C. Moïse, *J. Organomet. Chem.* **1989**, *364*, C3−C4. [2b] R. T. Baker, J. C. Calabrese, R. L. Harlow, I. D. Williams, *Organometallics* **1993**, *12*, 830−841. [2c] G. I. Nikonov, L. G. Kuzmina, P. Mountford, D. A. Lemenovskii, *Organometallics* **1995**, *14*, 3588−3591. [2d] G. Bonnet, O. Lavastre, J. C. Leblanc, C. Moïse, *New. J. Chem.* **1988**, *12*, 551−552. [2e] C. Poulard, G. Boni, P. Richard, C. Moïse, *J. Chem. Soc., Dalton Trans.* **1999**, 2725−2730. [2f] O. Lavastre, G. Bonnet, G. Boni, M. M. Kubicki, C. Moïse, *J. Organomet. Chem.* **1997**, *547*, 141−147. [2g] P. Sauvageot, O. Blacque, M. M. Kubicki, S. Juge, C. Moïse, *Organometallics* **1996**, *15*, 2399−2403. [2h] S. Challet, O. Lavastre, C. Moïse, J.-C. Leblanc, *New J. Chem.* **1994**, *18*, 1155−1161.

[3] G. A. A. Hadi, K. Fromm, S. Blaurock, S. Jelonek, E. Hey-Hawkins, *Polyhedron* **1997**, *16*, 721−731.
[4] P. J. Domaille, B. M. Foxmann, T. J. McNeese, S. S. Wreford, *J. Am. Chem. Soc.* **1980**, *102*, 4114−4120.
[5] J. B. Bonanno, P. T. Wolczanski, E. B. Lobkovsky, *J. Am. Chem. Soc.* **1994**, *116*, 11159−11160.
[6] C. C. Cummins, R. R. Schrock, W. M. Davis, *Angew. Chem.* **1993**, *105*, 758−761; *Angew. Chem. Int. Ed. Engl.* **1993**, *32*, 756−759.
[7] S. Blaurock, E. Hey-Hawkins, *Z. Anorg. Allg. Chem.*, in press.
[8] S. Blaurock, E. Hey-Hawkins, *Z. Anorg. Allg. Chem.* **2002**, *628*, 37−40.
[9] M. Culmsee, T. Kruck, G. Meyer, M. S. Wickleder, *Z. Anorg. Allg. Chem.* **2001**, *627*, 1111−1112.
[10] R. D. Sanner, S. T. Carter, W. J. Bruton, Jr., *J. Organomet. Chem.* **1982**, *240*, 157−162.
[11] E. Hey-Hawkins, S. Kurz, *Phosphorus, Sulfur, and Silicon* **1994**, *90*, 281−284.
[12] E. Hey-Hawkins, S. Kurz, J. Sieler, G. Baum, *J. Organomet. Chem.* **1995**, *486*, 229−235.
[13] C. Frenzel, E. Hey-Hawkins, *Phosphorus, Sulfur* **1998**, *143*, 1−17.
[14] E. Hey, F. Weller, *J. Chem. Soc., Chem. Commun.* **1988**, 782−783.
[15] U. Segerer, R. Felsberg, S. Blaurock, G. A. Hadi and E. Hey-Hawkins, Phosphorus, Sulfur **1999**, *144−146*, 477−480; S. Blaurock, *Dissertation*, Universität Leipzig, **2000**; S. Blaurock, G. A. Hadi, E. Hey-Hawkins, *Angew. Chem.* (in preparation).
[16] M. J. Bunker, A. de Cian, M. L. H. Green, J. J. E. Moreau, N. Siganporia, *J. Chem. Soc., Dalton Trans.* **1980**, 2155−2161.
[17] P. B. Hitchcock, M. F. Lappert, W. P. Leung, *Chem. Commun.* **1987**, 1282−1283.
[18] EI for **1−3**, FAB for **4a, 4b**. The mass spectra were recorded with a Varian MAT 711 (EI, 70 eV, source temperature 180 °C. FAB in nitrobenzaldehyde as matrix).
[19] [19a] J. A. M. Canich, F. A. Cotton, *Inorg. Chem.* **1987**, *26*, 3473−3478. [19b] F. A. Cotton, M. P. Diebold, W. J. Roth, *Polyhedron* **1985**, *4*, 1103−1108. [19c] A. J. Scioly, M. L. Luetkens, R. B. Wilson, J. C. Huffmann, A. P. Sattelberger, *Polyhedron* **1987**, *6*, 741−757. [19d] A. P. Sattelberger, R. B. Wilson Jr., J. C. Huffmann, *Inorg. Chem.* **1982**, *21*, 4179−4184. [19e] F. A. Cotton, M. P. Diebold, S. A. Duraj, W. J. Roth, *Polyhedron* **1985**, *4*, 1479−1484.
[20] L. Messerle, *Chem. Rev.* **1988**, *88*, 1229−1254.
[21] G. C. Campbell, J. A. M. Canich, F. A. Cotton, S. A. Duraj, J. F. Haw, *Inorg. Chem.* **1986**, *25*, 287−290.
[22] M. B. Hall, R. F. Fenske, *Inorg. Chem.* **1972**, *11*, 768−775.
[23] L. Pauling, *Die Natur der chemischen Bindung*, Verlag Chemie, Weinheim, **1962**.
[24] A. R. Chakravarty, F. A. Cotton, M. P. Diebold, D. B. Lewis, W. J. Roth, *J. Am. Chem. Soc.* **1986**, *108*, 971−976.
[25] R. J. Burt, G. J. Leigh, D. L. Hughes, *J. Chem. Soc., Dalton Trans.* **1981**, 793−799.
[26] V. C. Gibson, T. P. Kee, W. Clegg, *J. Chem. Soc., Dalton Trans.* **1990**, 3199−3210.
[27] [27a] D. W. Stephan, *Angew. Chem.* **2000**, *112*, 322−328; *Angew. Chem.* **2000**, *39*, 314−329. [27b] F. Mathey, *Multiple Bonds and Low Coordination in Phosphorus Chemistry*, M. Regitz, O. J. Scherer (eds), Thieme, Stuttgart, **1990**, p.38. [27c] F. Mathey, *Angew. Chem.* **1987**, *99*, 285−296; *Angew. Chem. Int. Ed. Engl.* **1987**, *26*, 275−286. [27d] K. D. Dillon, F. Mathey, J. F. Nixon, *Phosphorus: The Carbon Copy*, Wiley, Chichester, **1998**, p.19. [27e] M. J. M. Vlaar, A. W. Ehlers, F. J. J. de Kanter, M. Schakel, A. L. Spek, K. Lammertsma, *Angew. Chem.* **2000**, *112*, 3071−3074; *Angew. Chem. Int. Ed.* **2000**, *39*, 2943−2945. [27f] M. J. M. Vlaar, P. Valkier, A. W. Ehlers, F. J. J. de Kanter, M. Schakel, A. L. Spek, M. Lutz, K. Lammertsma, *Chem. Eur. J.* **2001**, *7*, 3551−3557. [27g] M. J. M. Vlaar, A. W. Ehlers, F. J. J. de Kanter, M. Schakel, A. L. Spek, M. lutz, N. Sigal, Y. Apeloig, K. Lammertsma, *Angew. Chem.* **2000**, *112*, 4296−4299; *Angew. Chem. Int. Ed.* **2000**, *39*, 4127−4130. [27h] M. J. M. Vlaar, F. J. J. de Kanter, M. Schakel, A. L. Spek, M. Lutz, K. Lammertsma, *J. Organomet. Chem.* **2001**, *617−618*, 311− 317. [27i] M. J. M. Vlaar, S. G. A. van Assema, F. J. J. de Kanter, M. Schakel, A. L. Spek, M. Lutz, K. Lammertsma, *Chem. Eur. J.* **2002**, *8*, 58−65. [27j] M. J. M. Vlaar, A. W. Ehlers, M. Schakel, S. B. Clendenning, J. F. Nixon, M. Lutz, A. L. Spek, K. Lammertsma, *Chem. Eur. J.* **2001**, *7*, 3545−3549. [27k] J. B. M. Wit, G. Th. van Eijkel, F. J. J. de Kanter, M. Schakel, A. W. Ehlers, M. Lutz, A. L. Spek, K. Lammertsma, *Tetrahedron* **2000**, *56*, 137−141. [27l] J. B. M. Wit, G. Th. van Eijkel, F. J. J. de Kanter, M. Schakel, A. W. Ehlers, M. Lutz, A. L. Spek, K. Lammertsma, *Angew. Chem.* **1999**, *111*, 2716−2719; *Angew. Chem. Int. Ed.* **1999**, *38*, 2596−2599. (and references therein)
[28] [28a] P. Jernakoff, C. de Meric de Bellefon, G. L. Geoffroy, A. L. Rheingold, S. J. Geib, *Organometallics* **1987**, *6*, 1362−1364. [28b] H.-J. Gosink, H. W. Roesky, H.-G. Schmidt, M. Noltemeyer, E. Irmer, R. Herbst-Irmer, *Organometallics* **1994**, *13*, 3420−3426. [28c] E. Benory, A. Bino, D. Gibson, F. A. Cotton, Z. Dori, *Inorg. Chim. Acta* **1985**, *99*, 137−142. [28d] D. T. Richens, L. Helm, P.-A. Pittet, A. E. Merbach, F. Nicolõ, G. Chapuis, *Inorg. Chem.* **1989**, *28*, 1394−1402. [28e] F. Boutonnet, M. Zablocka, A. Igau, J. Jaud, J.-P. Majoral, J. Schamberger, G. Erker, S. Werner, C. Krüger, *J. Chem. Soc., Chem. Commun.* **1995**, 823−824. [28f] J. de la Mata, R. Fandos, M. Gómez, P. Gómez-Sal, S. Martinez-Carrera, P. Royo, Organometallics **1990**, *9*, 2846−2850. [28g] N. Wiberg, *Lehrbuch der Anorganischen Chemie*, Walter de Gruyter & Co., Berlin, **1985**.
[29]]M. Baudler, K. Glinka, *Chem. Rev.* **1993**, *93*, 1623−1667.
[30] N. Etkin, M. T. Benson, S. Courtenay, M. J. McGlinchey, A. D. Bain, D. W. Stephan, *Organometallics* **1997**, *16*, 3504−3510.
[31] M. Yoshifuji, I. Shima, N. Inamoto, K. Hirotsu, T. Higuchi, *J. Am. Chem. Soc.* **1981**, *103*, 4587−4589.
[32] [32a] J. C. Green, M. L. H. Green, G. E. Morris, *J. Chem. Soc., Chem. Commun.* **1974**, 212−213. [32b] P. S. Elmers, M. L. Scudder, B. O. West, *J. Organomet. Chem.* **1976**, *122*, 281−288. [32c] B. Deppisch, H. Schäfer, *Acta Crystallogr., Sect. B* **1982**, *38*, 748−751. [32d] M. M. Olmstead, P. P. Power, *J. Am. Chem. Soc.* **1984**, *106*, 1495−1496. [32e] J. Chatt, P. B. Hitchcock, A. Pidcock, C. P. Warrens, K. R. Dixon, *J. Chem. Soc., Chem. Commun.* **1982**, 932−933. [32f] A. H. Cowley, J. E. Kilduff, J. G. Lasch, N. C. Norman, M. Pakulski, F. Ando, T. C. Wright, *Organomet.* **1984**, *3*, 1044−1050. [32g] S. Kurz, E. Hey-Hawkins, *J. Organomet. Chem.* **1993**, *462*, 203−207.
[33] M. Baudler, J. Hahn, H. Dietsch, G. Fürstenberg, *Z. Naturforsch., Teil B* **1976**, *31*, 1305−1310.
[34] [34a] M. Baudler, B. Carlsohn, W. Böhm, G. Z. Reuschenbach, *Z. Naturforsch., Teil B* **1976**, *31*, 558−564. [34b] M. Baudler, G. Reuschenbach, *Z. Anorg. Allg. Chem.* **1980**, *464*, 9−16.
[35] M. Baudler, B. Carlson, D. Koch, P. K. Medda, *Chem. Ber.* **1978**, *111*, 1210−1216.
[36] [36a] G. Becker, M. Rössler, E. Schneider, *Z. Anorg. Allg. Chem.* **1978**, *439*, 121−133. [36b] C. Frenzel, *Dissertation*, Universität Leipzig, **1999**.
[37] SHELXTL PLUS, Siemens Analyt. X-ray Inst. Inc., **1990**, XS: *Program for Crystal Structure Solution*, XL: *Program for Crystal Structure Determination*, XP: *Interactiv Molecular Graphics.*
[38] R. H. Blessing, *Acta Crystallogr., Sect. A* **1995**, *51*, 33−38.
[39] S. Kurz, *Dissertation*, Universität Leipzig, **1994**.
[40] D. Feitler, G. M. Whitesides, *Inorg. Chem.* **1976**, *15*, 466−469.
[41] A. Cowley, N. C. Norman, M. Pakulski, *Inorg. Syn.* **1990**, *27*, 235−240.

Received March 15, 2002
[I02138]